J Nanopart Res (2021) 23: 82
https://doi.org/10.1007/s11051-021-05200-w

RESEARCH PAPER

Electrochemical determination of amlodipine using a CuO-NiO nanocomposite/ionic liquid modified carbon paste electrode as an electrochemical sensor

Mahzad Firouzi · Masoud Giahi · Mostafa Najafi · Seyed Saied Homami · Seyed Husain Hashemi Mousavi

Received: 28 December 2020 / Accepted: 23 March 2021 / Published online: 30 March 2021

Abstract In this paper, a nanocomposite of CuO-NiO was synthesized by sol-gel method. Its structure and morphology were characterized by X-ray diffraction, field emission scanning electron microscopy (FESEM), and energy-dispersive X-ray spectroscopy techniques. The FESEM image showed particles with the size at about 30–80 nm in diameters. In continue, a carbon paste (CP) modified electrode with CuO-NiO nanocomposite and an ionic liquid ((1-butyl-3-methylimidazolium hexafluorophosphate (BMIM-PF_6)) (CuO-NiO/IL/CPE) was fabricated as an electrochemical sensor for determination of amlodipine (AML). The cyclic and differential pulse voltammetry, electrochemical impedance spectroscopy, and chronoamperometry were used for electrochemical studies and AML determination. The CuO-NiO/IL/CPE indicated a good electrocatalytic behavior towards to oxidation of AML. The anodic peak currents were increased with the AML concentration and indicated a linear dynamic range from 0.1 to 100 μM and a detection limit of 0.06 μM (S/N = 5) under the optimized conditions. The introduced electrochemical sensor was utilized for the determination of AML in the pharmaceutical formulations, human urine, and blood plasma samples.

M. Firouzi · M. Giahi (✉) · S. S. Homami · S. H. H. Mousavi
Department of Chemistry, South Tehran Branch, Islamic Azad University, Tehran, Iran
e-mail: m_giahi@azad.ac.ir

M. Najafi (✉)
Department of Chemistry, Faculty of Science, Imam Hossein University, Tehran, Iran
e-mail: mnajafi@ihu.ac.ir

Keywords Amlodipine · Ionic liquid · BMIM-PF_6 · Voltammetry · CuO-NiO · Nanocomposite · CuO-NiO/IL/CPE · Pharmacokinetic study · Electrocatalytic behavior

Introduction

Hypertension can led to risk of serious problem such as stroke, heart disease, aneurysm, and sometimes death. Most of the people with hypertension need treatment with antihypertensive drugs such as losartan (LOS), valsartan (VAL), and AML. AML (3-ethyl-5-methyl-2-[aminoethoxy-methoxy]-4-(o-chlorophenyl)-1, 4-dihydro-6-methyl-3,5-pyridinedicarboxylate monobenzene sulfonate) has been used with or without other medication to treat high blood pressure (Dollery 1999; Kearney et al. 2005). AML is a calcium channel blocker drug. It acts by relaxing blood vessels so blood can flow more easily. Also, it can be used to treat coronary heart failure and chest pain (Choi et al. 2014; Fares et al. 2016). Different analytical techniques including chromatography (Shaikh et al. 2020), high-performance chromatography tandem mass spectrometry (HPLC/MS) (Chen et al. 2018), LC/MS/MS (Johannsen et al. 2019), and spectrophotometry (Attala and Elsonbaty 2021) have been applied to determine AML in pharmaceutical drugs and biological samples. The HPLC technique recommended as an official method for the individual determination of AML in the United States pharmacopeia (United States Pharmacopoeia 2009). The chromatographic-based

methods need the use of organic solvents, time-consuming derivitization steps, and extensive preliminary sample pretreatment. Electrochemical methods have gained including easy to operate, rapid, economical, sensitive, short analysis time, and inexpensive production. Various electrochemical sensors have been reported for AML sensing in the pharmaceutical formulations and biological samples such as gold electrode (Stoiljković et al. 2012), pencil graphite electrode (Jadon et al. 2017), boron-doped diamond (BDDE) (Švorc et al. 2014), edge plane pyrolytic graphite electrodes (EPPGE) (Goyal and Bishnoi 2010), TiO_2 modified CPE (Erden et al. 2016), and $NiMoO_4$/chitosan nanocomposite modified GCE (Lou et al. 2020).

Ionic liquids due to good chemical and thermal stability, low vapor pressure, and high ionic conductivity have been used to make various modified electrodes (Opallo and Lesniewski 2011; Mohammadi et al. 2017). They could decrease the overpotential and enhance the electrochemical signal of analytes. In recent years, metal oxide nanostructures have received much attention in many fields, such as photocatalyst (Reddy et al. 2020), chemical and electrochemical sensors (Chen et al. 2008; Naghian and Najafi 2018), and gas sensor (Mirzaei et al. 2016) because of their large surface area, catalytic effect, and chemical stability.

In the present work, combining the advantages of ionic conductivity of ionic liquid ($BMIM.PF_6$), large surface area, and catalytic effect of metal oxide nanostructures (CuO-NiO) was used to develop a CP modified electrode (CuO-NiO/IL/CPE) for the determination of AML in human urine and blood plasma samples. The experimental parameters were optimized, and the sensor was used to determine of the AML in real samples. Some advantages of this work are simplicity, rapidity, being operative, cheap, and easy to usage for AML determination.

Experimental

Materials

Graphite powder (extra pure, particle size < 50 μm), hydrochloric acid, sodium hydroxide, tetramethyl ammonium hydroxide (TMAH), copper (II) sulfate pentahydrate ($CuSO_4.5H_2O$), nickel (II) acetate tetra hydrate ($Ni(CH_3CO_2)_2.4H_2O$), and mineral oil were purchased from Merck. AML (as besylate, purity: 98.7%) was obtained from ARYA Pharmaceutical Co., Iran. The commercial tablets labeled Amelodipin 5 mg and Amlodipine:Valsartan (AML:VAL) tablets labeled 5:80 mg were purchased from local drugstore.

Apparatus

All voltammetric measurements were recorded using an Autolab potentiostat/galvanostat type 302N (Metrohm, The Switzerland) controlled by NOVA software version 2.1.2. A conventional three-electrode system consisted of a bare or modified CPE as working electrode and an Ag/AgCl and a Pt wire as the reference and auxiliary electrode, respectively. A Metrohm-481 pH-meter (Switzerland) was used for pH adjustments. The morphology of the synthesized nanocomposite was analyzed with field emission scanning electron microscope (FESEM) (Zeiss Co., Sigma, Germany) equipped with an energy-dispersive X-ray spectrometer (EDX) (Zeiss Co., Ultra Plus, Germany). Gold coating of thickness (approximately) 8 nm at 10 mA for 60 s was carried out on sample using sputter coater before FESEM imaging. The X-ray diffraction (XRD) pattern was recorded by an X-pertpro (Panalytical, Netherlands) and operated at 40 KV and 40 mA with λ = 1.5406 Å in the 2θ range of 10°–90°.

Synthesis of the CuO-NiO nanocomposite

CuO-NiO nanocomposite was prepared by the sol-gel method. First, 0.5 g of $Ni(CH_3CO_2)_2.4H_2O$ was dissolved in 20 ml of distilled water. Then, 0.5 g of citric acid was added and stirred at 65 °C. In continue, NaOH (1 M) was added dropwise to the solution until a highly viscous gel precursor is formed. In the next step, 50 ml of $CuSO_4.5H_2O$ (0.2 M) and 1 ml of CH_3COOH were mixed in a 100 ml PYREX beaker and heated until boil. Then, a few drop of NaOH (2 M) was added to the solution, so that a pH of 11–12 was achieved, and the $Cu(OH)_2$ was precipitate. The blue $Cu(OH)_2$ precipitate was slowly changing into black precipitate CuO and boiled for 2 h. The precipitate was washed with ethanol and distilled water by centrifugation until all NaOH is eliminated. The precipitate of CuO and gel of NiO were transferred to a 100 ml beaker containing 20 ml of distilled water and stirred for 10 min. Then, the mixture is sonicated for 30 min after adding the TMAH solution (7.5 ml, 0.28 M). The mixture was additionally sonicated for 30 min, and end of the step was added TMAH

(7.5 ml, 0.28 M). The precipitate is filtered and dried in an oven at 80 °C for 24 h. The dried precipitate was then calcined in a muffle furnace at 600 °C for 3 h.

Preparation of modified electrodes

The CuO-NiO/IL/CPE was fabricated by mixing the 0.37 g of graphite powder, 0.03 g of CuO-NiO, 30 μL of BMIM.PF_6, and 0.10 g of mineral oil. The fabricated pastes were packed inside a poly-amide tube (inner diameter 2.5 mm), and the electrical contact with a copper wire was provided. Before use, the surface of CuO-NiO/IL/CPE was smoothed on a piece of polishing paper. The conventional CPE was fabricated by mixing of 0.40 g of graphite powder and 0.10 g of mineral oil in a mortar and pestle. The IL/CPE modified electrode was fabricated by mixing of 0.40 g of graphite powder, 30 μl of BMIM.PF_6, and 0.10 g of mineral oil, and the CuO-NiO/CPE modified electrode was prepared by mixing the 0.37 g of graphite powder, 0.03 g of CuO-NiO, and 0.10 g of mineral oil.

Electrochemical measurements

A stock solution of AML (1 mM) was prepared in methanol. AML working solution was daily prepared by dilution of this stock solution with the phosphate buffer (PB) before use. The PB (0.1 M) was used as supporting electrolyte and was prepared by mixing $Na_2HPO_4.2H_2O$ (0.2 M) and $NaH_2PO_4.H_2O$ (0.2 M). The pH of PB was adjusted using NaOH (0.2 M) and HCl (0.1 M).

The electrochemical properties of the CPE and modified electrodes were investigated in $K_4[Fe(CN)_6]$ (5 mM) and KCl (0.1 M) solution by cyclic voltammetry (CV) and electrochemical impedance spectroscopy (EIS) techniques. The CVs were recorded between 0 and 0.8 V at a scan rate range from 5 to 100 mV s^{-1}. EIS measurements were recorded in the potential amplitude of 10 mV and a frequency amplitude of 0.1 to 10^5 Hz in $K_4[Fe(CN)_6]$ (5 mM) and KCl (5 mM). Electrochemical behaviors and determination of AML were studied by differential pulse voltammetry (DPV) and chronoamperometric (CA) methods. DPV was used at a potential range from 0.3 to 0.7 V, and chronoamperometric responses were recorded at a potential step 0.7 V. All measurements were carried out in triplicate for each concentration.

Analysis of real sample

AML and AML:VAL are available in tablet form for oral administration containing the equivalent to 5 and 5:80 mg as AML base. Ten tablets (AML ARYA 5 from ARYA Pharmaceutical Co. and Valzomix 5/80MG TAB from Dr. Abidi Pharmaceutical Labs.) were accurately weighed and powdered in a mortar. An adequate amount of the finely powdered tablet was dissolved in 5 ml methanol and sonicated for 5 min. Then, the solution was filtered and transferred into a 5 ml volumetric flask and diluted to mark by methanol to obtain a final solution containing 0.00176 M AML. Required volumes to prepare each concentration were transferred into a 10 ml volumetric flask and diluted with PB (0.1 M). The prepared transferred to the electrochemical cell just prior to electrochemical analysis.

A human urine sample of 10 ml was stored in the refrigerator; 5 ml of urine was centrifuged (10 min at 1500 rpm) and diluted with PB (0.1 M, pH 9) in a ratio of 1:2 and was used for AML determination by standard addition method. Human blood plasma was prepared from Iranian Blood Transfusion Organization and stored in the centrifuged. The sample was centrifuged (2 min at 2000 rpm), and then 4 ml of methanol was added to precipitate the proteins, and the clear supernatant layer was filtrated. The free protein human blood plasma was diluted with PB (0.1 M, pH 9) in a 10 ml volumetric flask and was used for AML determination by standard addition method.

Results and discussion

Characterization

The FESEM was utilized to evaluate the morphology of the CuO-NiO nanocomposite (gold coated) as indicated in Fig. 1a. Figure 1a shows that the synthesized CuO-NiO nanocomposite is uniform in particle size (at about 30–80 nm in diameters) and has rice shape with some agglomeration. The composition of the sample is evaluated by EDS analysis (Fig. 1b) which shows Cu, Ni, and O elements in composition without any appreciable impurities.

The XRD pattern of the CuO-NiO nanocomposite is displayed in Fig. 1c. In this figure, the presence of CuO and NiO were clearly revealed by the characteristic diffraction peaks. The diffraction peaks at 32.51°,

35.57°, 38.68°, 43.31°, 46.27°, 48.83°, 53.32°, 58.23°, 59.14°, 60.2°, 66.4°, and 66.23° are related to the CuO monoclinic tenorite phase and have agreement with the standard card (JCPDS no. 01-080-0076). The other diffraction peaks at 37.08°, 43.29°, and 64.23° are related to the face-centered-cubic structure of NiO and standard card of JCPDS no. 01-078-0423. The average crystalline size of the CuO-NiO nanocomposite was calculated to be 75.4 nm by the Debye–Scherrer equation (Eq. 1):

$$D = \frac{k\lambda}{\beta \cos\theta} \tag{1}$$

where D is the crystallite size (nm), k is a constant (0.94 for spherical particles), λ is the wavelength of the X-ray radiation (Cu-Kα = 0.1541 nm), β is the full width at half maximum (FWHM) of the intense and broad peaks, and θ is the Bragg's or diffraction angle.

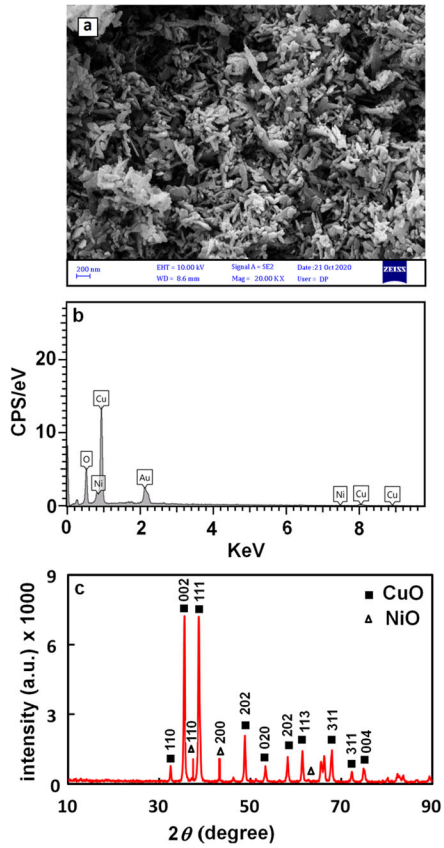

Fig. 1 **a** FESEM image of CuO-NiO nanocomposite. **b** EDS spectra of CuO-NiO nanocomposite. **c** XRD patterns of CuO-NiO nanocomposite

Electrochemical properties of working electrodes

The CVs of the CPE, CuO-NiO/CPE, IL/CPE, and CuO-NiO/IL/CPE in the $K_4Fe(CN)_6$ (5 mM) and KCl (0.1 M) at the scan rate of 50 mV s^{-1} are shown in Fig. 2a. As can be seen, the anodic and cathodic peaks corresponding to $K_4Fe(CN)_6$ for the modified electrodes CuO-NiO/IL/CPE (Trace d) are significantly increased related to CPE (Trace a). On the other hand, the peak separations (ΔE_p) are obtained at 0.33, 0.29, 0.29, and 0.26 V for CPE, CuO-NiO/CPE, IL/CPE, and CuO-NiO/IL/CPE, respectively. The obtained results indicate a good improvement in the electron transfer kinetic at the surface of the CuO-NiO/IL/CPE.

The Nyquist diagrams of the CPE, CuO-NiO/CPE, IL/CPE, and CuO-NiO/IL/CPE were recorded in $K_4Fe(CN)_6$ (5 mM) solution with the frequencies swept from 0.1 to 10^5 Hz, and the results are shown in Fig. 2b. The charge transfer resistances of the electrodes were estimated by fitting of the impedance spectra to the well-known Randles equivalence circuit model. The R_{ct} values of the CPE, CuO-NiO/CPE, IL/CPE, and CuO-NiO/IL/CPE were found to be the order of Rct are 950, 850, 140 and 658400, 9500, 140, and 65 Ω, respectively. The low charge resistance value observed at the surface of the CuO-NiO/IL/CPE clearly indicates that the presence of CuO-NiO and $BMIM.PF_6$ can effectively accelerate the electron transfer rate of redox reactions. The effective surface area (A) was calculated for the electrodes by the Randles–Sevcik (Bard and Faulkner 2001) equation (Eq. 2):

$$I_{pa} = \left(2.69 \times 10^5\right) n^{2/3} A D^{1/2} v^{1/2} C \tag{2}$$

where I_{pa} is the peak current, A is the surface area of the electrode, n is the electron number, is the scan rate, and D and C are the diffusion coefficient and concentration of $K_4Fe(CN)_6$. The effective surface area values found for the electrodes were 0.08 cm^2 (CPE) and 0.32 cm^2 (CuO-NiO/IL/CPE). This is mainly attributed to much higher redox currents and improved sensitivity of CuO-NiO/IL/CPE.

Electrochemical behavior of AML

The electrochemical behavior of AML was investigated at surface of CPE, CuO-NiO/CPE, IL/CPE, and CuO-NiO/IL/CPE in PB (0.1 M, pH 9) and scan rate of 50 mV s^{-1} (Fig. 3). In this figure, the scans a, b, c, and

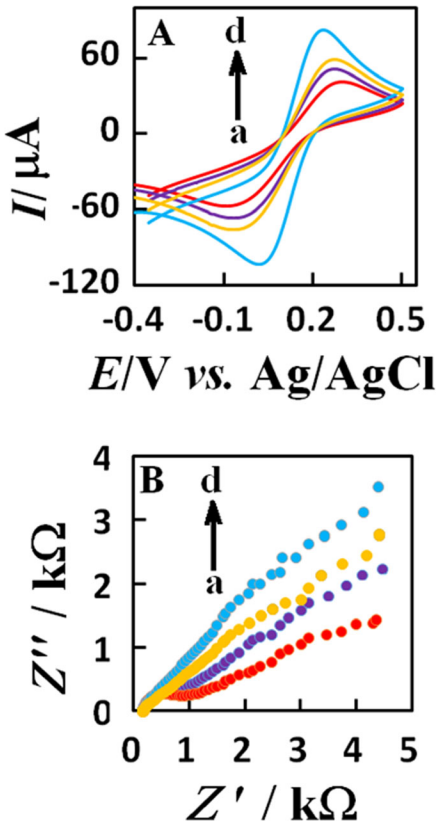

Fig. 2 **a** CVs and **b** EIS of CPE (a), CuO-NiO/CPE (b), IL/CPE (c), and CuO-NiO/IL/CPE (d) in the presence of $K_4Fe(CN)_6$ (5 mM) and KCl (0.1 mM) solution with the scan rate of 50 mV/s. EIS condition: frequency range: 0.1 to 10^5 Hz; perturbation amplitude: 10 mV

d show the cyclic voltammograms of CPE, CuO-NiO/CPE, IL/CPE, and CuO-NiO/IL/CPE, respectively. At the CuO-NiO/IL/CPE, the oxidation of AML occurs with a peak potential of nearly 0.55 V (vs. Ag/AgCl as reference electrode), while the oxidation of AML on the CPE, CuO-NiO/CPE, and IL/CPE gives peaks at about 0.58, 0.59, and 0.59 V (Fig. 3, curves a, b, and c). Also, the anodic peak current is increased at CuO-NiO/IL/CPE, and the lowest onset potential for electrooxidation of AML is about 0.25 V in compare with about 0.45 V for other electrodes. These results are clear indications for the occurrence of an electrocatalytic process at surface of CuO-NiO/IL/CPE.

Effect of pH

The effect of pH on oxidation of AML at 100 μM concentration was investigated in the range of pH 4–9 by CV (Fig. 4a). As can be seen, with the increase of pH solution, the peak potential shifted to less positive values and the oxidation peak current increased. The relationships between peak potential (E_p) and pH provided by the equation: E_p (V) = − 0.0557 pH + 1.0338 (R^2 = 0.9898) (Fig. 4b). The slope value from the data was obtained 55.7 mV/pH. This value was indicated equal numbers of electrons and protons contributed in the electrooxidation process. On the other hand, the oxidation peak current is increased by the increasing of pH solution from 4 to 8, and it achieves a maximum at about pH 8 and 9. Therefore, PB (0.1 M, pH 9) was utilized as optimum pH in all voltammetric measurements because of the potential shifted to less positive value.

.

Effect of scan rate

The influence of scan rate ( ) on the oxidation peak current of AML (100 μM) at surface of CuO-NiO/IL/CPE was studied by CV in the range of 5 to 100 mV s^{-1}. As shown in Fig. 5a, the oxidation currents increased gradually with the increase of the scan rate. The oxidation peak currents showed a linear relationship with the square root of scan rate (I_{pa} (μA) = 0.86 $^{1/2}$ mV s^{-1} − 1.27 with a correlation of R^2 = 0.9905) (inset a), demonstrating a diffusion-controlled process. The peak potential (E_p) of the oxidation wave was observed to shift anodically with increasing sweep rate.

Tafel plot was drawn from points of the tafel region of the voltammogram at scan rate of 5 mV s^{-1} to obtain information on the rate determining step. The tafel slope

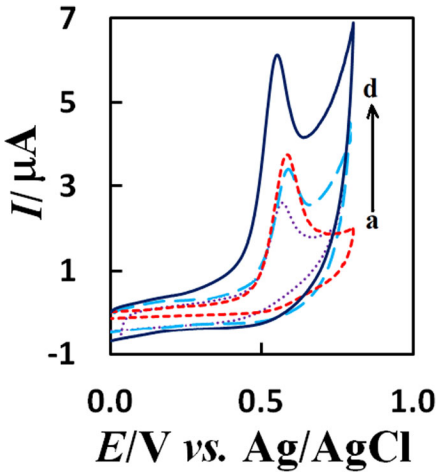

Fig. 3 CVs of (a) CPE, (b) CuO-NiO/CPE, (c) IL/CPE, and (d) CuO-NiO/IL/CPE in PB (0.1 M, pH 9) containing AML (100 μM) at scan rate of 50 mV/s

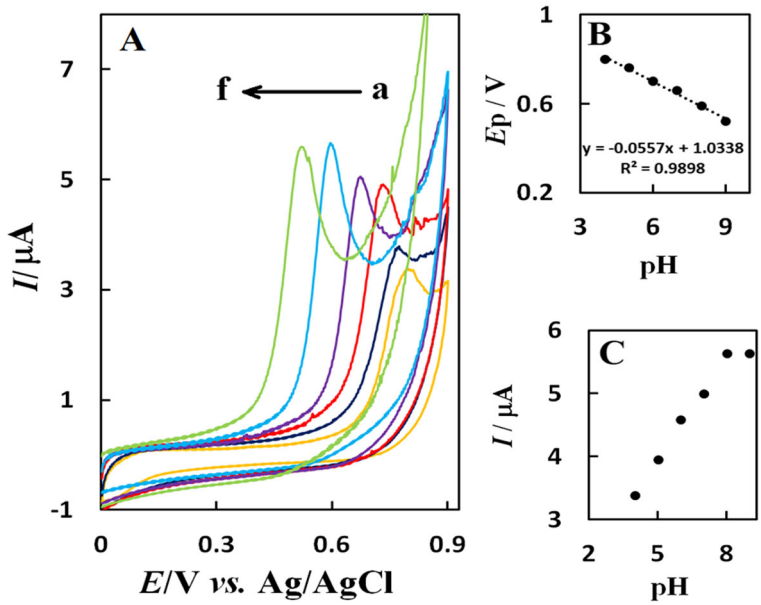

Fig. 4 **a** CVs of 100 µM AML on CuO-NiO/IL/CPE at different pH values (a to f are 4, 5, 6, 7, 8, and 9, respectively. The scan rate was 50 mV/s. **b** The relationship between the peak potential (E_p) and pH. **c** The relationship between the oxidation peak current (I_{pa}) and pH

of 0.1248 V obtained from Fig. 5b agrees with the involvement of one electron in the rate-determining step for the electrooxidation of AML, assuming a charge transfer coefficient of α = 0.52. The charge transfer coefficient also could be calculated from Fig. 5c and Eq. 3 by another method introduced by Andrieux and Saveant (Andrieux and Saveant 1978):

$$E_p = b/2 \log(v) + K \quad (3)$$

where b is the tafel slope and the intercept of the plot of E_p vs. log v is constant. The slope of the linear regression is equal to $b/2 = 0.059/(1 - \text{-})n$. Thus, b is $2(0.059/(1 - \text{-})n)$. The tafel slope (b) was 0.058 V and by considering that α equals 0.49. The result is in agreement with previous mentioned method. Based on the obtained results, the electrochemical oxidation mechanism of AML at CuO-NiO/IL/CPE can occur by releasing two electrons and two protons according to Fig. 6.

Chronoamperometry measurement

The catalytic oxidation of AML by CuO-NiO/IL/CPE is evaluated by choronoamperometry (CA). Figure 7a indicates the chronoamperograms recorded at the potential step of 0.7 V. These chronoamperograms have been used for the determination of diffusion coefficient of AML. The diffusion coefficient of AML was calculated by the Cottrell equation (Bard and Faulkner 2001) (Eq. 4):

$$I_{pa} = n\ F\ A\ C\ D^{1/2}\ \pi^{-1/2}\ t^{-1/2} \quad (4)$$

where I_{pa} is the current, F is the Faraday constant, n is number of electrons (n = 2 for AML electrooxidation), D is the diffusion coefficient, C is the analyte concentration, t is the time, and A is the geometrical area (0.32 cm^{-2}). The various concentrations for AML (0.05–0.2 mM) were utilized in this investigation. Linear plots of I_{pa} vs. $t^{-1/2}$ were employed for various concentration of AML (Fig. 7a, inset a). Figure 7a, inset b, exhibits the fitted experimental plots for various concentrations of the AML. The diffusion coefficient (D) was obtained to be 2.1×10^{-6} for AML. The catalytic rate constant (K_{cat}) between AML and CuO-NiO/IL/CPE was calculated by the method described in the literature (Bard and Faulkner 2001) (Eqs. 5 and 6):

$$\frac{I_{cat}}{I_L} = \lambda 1/2 \left[\pi 1/2\ \text{erf}\ (\lambda 1/2) + \frac{\exp(-\lambda)}{\lambda^{1/2}}\lambda\right. = k\text{cat}\ C_o\ t \quad (5)$$

$$\frac{I_{cat}}{I_l} = \pi^{1/2}\ (K\text{cat}\ C_o\ t)^{1/2} \quad (6)$$

where I_{cat} and I_d are the currents of CuO-NiO/IL/CPE in the presence and in the absence of AML. The K_{cat} was calculated to be 5.2×10^3 cm^3 mol^{-1} s^{-1} from Fig. 7b.

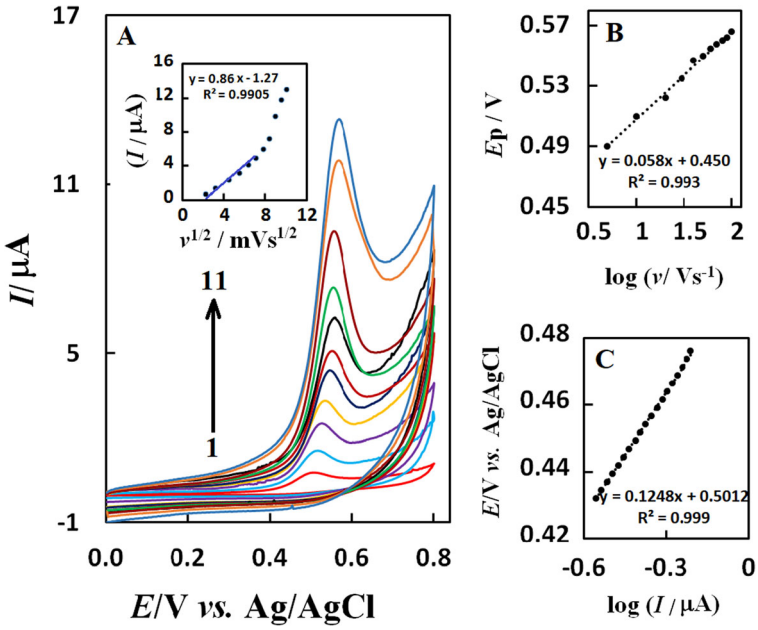

Fig. 5 **a** Cyclic voltammograms of AML (100 μM) on CuO-NiO/IL/CPE in PB (0.1 M, pH 9) with different scan rates ( ): (Andrieux and Saveant 1978) 5, (Attala and Elsonbaty 2021) 10, (Arvand et al. 2021) 20, (Bard and Faulkner 2001) 30, (Beitollahi et al. 2016) 40, (Chen et al. 2008) 50, (Chen et al. 2018) 60, (Choi et al. 2014) 70, (Dogan-Topal et al. 2009) 80, (Dollery 1999) 90, and (Doulache et al. 2020) 100 mV/s. Inset: linear dependence of I_p versus square root of the scan rate. **b** The tafel plot derived from the CV at scan rate of 5 mV/s. **c** Plot of E_p vs. log (v)

Determination of AML

DPV was used for the AML determination, and the related voltammograms are shown in Fig. 8a. As can be seen, the oxidation peak currents increased linearly with increasing AML concentration in the range from 0.1 to 100 μM. The linear regression equation was I (μM) = 0.0382 + 0.9292 C (μM) with the correlation coefficient of 0.9944 (Fig. 8b). From the analysis of these data, the limit of detection (LOD) was calculated to be 0.06 μM based on the signal-to-noise ratio (S/N) of 5. Some characteristics of the CuO-NiO/IL/CPE compared with other reported voltammetric methods are shown in Table 1. The different voltammetric methods for determination of AML are reported in Table 1. The LOD and calibration range for AML determination of this work are comparable and or better than those obtained by other reports. Also, the constructed CuO-NiO/IL/CPE is cheaper and simpler than that of many other modified electrodes reported in literature.

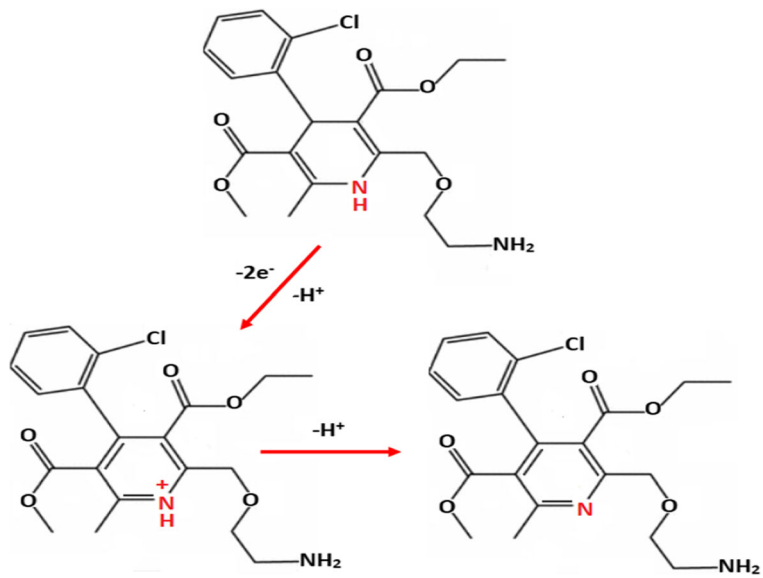

Fig. 6 Electrooxidation mechanism of AML

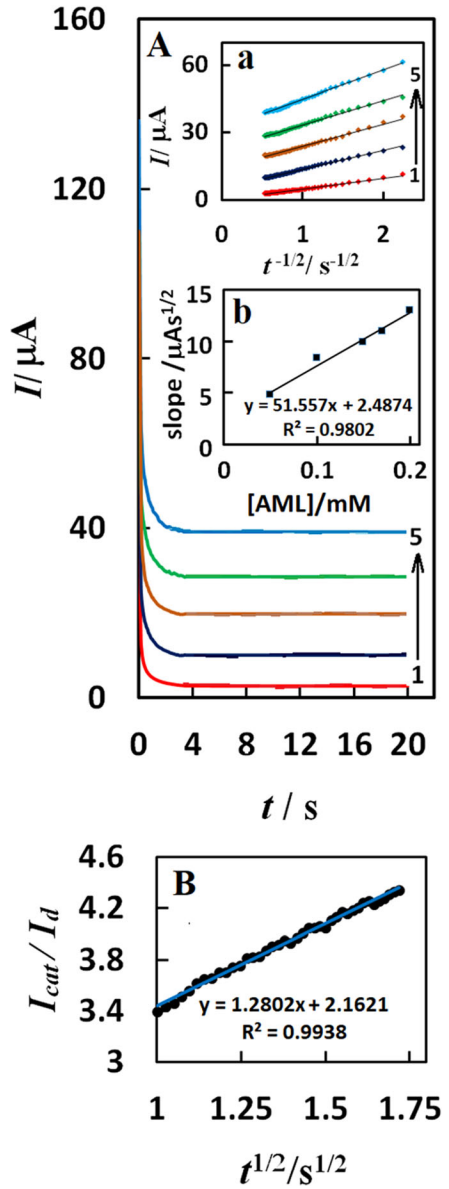

Fig. 7 **a** Chronoamperometric response of the CuO-NiO/IL/CPE in PB (0.1 M, pH 9) for different concentration of AML (0.05–0.2 mM) for a potential step of 0.7 V Ag/AgCl. The traces of 1 to 5 correspond to 0.05 to 0.2 mM of AML. Inset 7(a) Plots of I vs. $t^{1/2}$ obtained from chronoamperograms 1–5. Inset 7(b) Plot of the slope of the straight lines against the AML concentration 1–5. **b** The plot of I_{cat}/I_d vs. $t^{1/2}$ from chronoamperometric for 0.05 mM of AML

Interference study

The selectivity of the CuO-NiO/IL/CPE for AML with some different substances as interfering compounds was investigated. The interference study was examined by DPV current responses in the solution mixture containing AML (100 µM) and PB (0.1 M, pH 9). Ascorbic acid (AA) is one of the main metabolites existing in the human urine. Therefore, simultaneous detection of AML and AA was checked (Fig. 9a). As seen, AA has no interference in AML determination. The hydrochlorothiazide (HCTZ) and VAL are used for treatment of hypertension separately or together in a combined pharmaceutical formulation. Figure 9b shows the DPV of a solution containing AML (100 µM), HCTZ (100 µM), and VAL (100 µM) at surface of CuO-NiO/IL/CPE. The result indicated that oxidation of HCTZ and VAL is occurred in potential peaks of 0.76 and 1.3 V respectively and no interference on oxidation of AML.

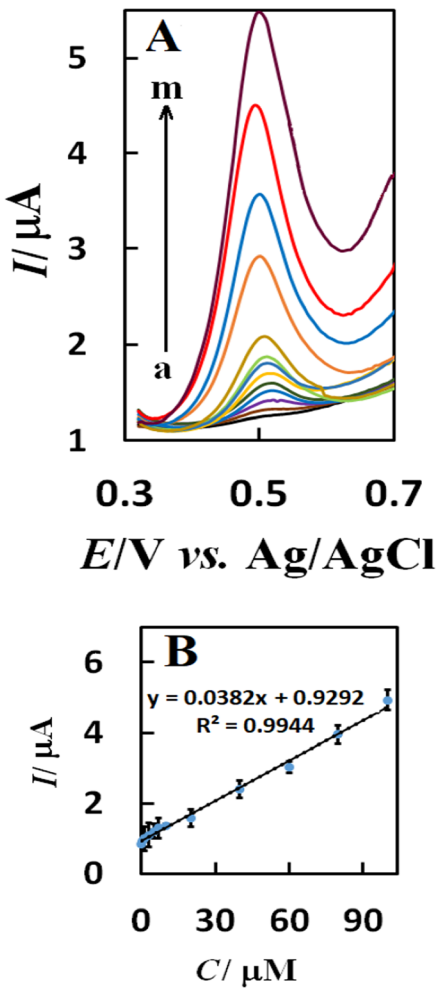

Fig. 8 **a** DPVs of CuO-NiO/IL/CPE in the solution containing AML at different concentrations: (a) 0, (b) 0.1, (c) 0.5, (d) 1, (e) 3, (f) 5, (g) 7, (h) 10, (i) 20, (g) 40, (k) 60, (l) 80, and (m) 100 µM, respectively. **b** The relationship of the anodic peak current with the AML concentration

Table 1 The comparison of different methods for AML determination

Electrode	Technique	Linear range	LOD	Ref.
MWCNT/gold electrode	SWASV[a]	24–34 μM	4.2 μM	(Stoiljković et al. 2012)
Pencil graphite electrode	DPV	0.8–51.2 nM	0.04 pM	(Jadon et al. 2017)
Boron-doped diamond electrode	DPV	6–38 μM	0.07 μM	(Švorc et al. 2014)
TiO_2/CPE	SWASV	0.01–1 μM	0.00297 μM	(Erden et al. 2016)
$NiMoO_4$/CHIT/GCE	DPV	0.1–374.5 μM	12.74 nM	(Lou et al. 2020)
Fe_3O_4@SiO_2/MWCNT/IL/CPE	SWV	0.25–500 μM	0.15 μM	(Beitollahi et al. 2016)
GCE	DPV	4–100 μM	0.8 μM	(Dogan-Topal et al. 2009)
GCE	DPV	1–35 μM	0.31 μM	(Erden et al. 2014)
ZrO_2/GCE	DPV	10–200 μM	2 μM	(Mohammadizadeh et al. 2017)
GNRs-GO-fCNTs/GCE[b]	DPV	0.01–1 1–75 μM	3 nM	(Arvand et al. 2021)
Poly (Gly)/GCE[c]	DPAdSV[d]	0.5–25 μM	0.08 μM	(Doulache et al. 2020)
M-CeO_2-HSs/GCE[e]	DPV	0.001–400 μM	7.9 nM	(Farvardin et al. 2020)
Pt-NiO/MWCNTs/GCE	DPV	1–250 μM	0.092 μM	(Dehdashti and Babaei 2020)
fMWCNT/CuNPs-CPE	AdSWV[f]	2.0×10^{-8} to 6.3×10^{-6} M	5.16×10^{-10} M	(Naikoo et al. 2020)
CuO-NiO/IL/CPE	DPV	0.1-100 μM	0.06 μM	This work

[a] Square-wave anodic stripping voltammetry

[b] Gold nanorods-graphene oxide functionalized carbon nanotubes nanocomposite coated glassy carbon electrode

[c] Polyglycine

[d] Differential pulse adsorptive stripping voltammetric

[e] Mesoporous CeO_2 hollow spheres

[f] Adsorptive square wave voltammetry

Precision, stability, and reproducibility

The precision of the method was estimated in terms of relative standard deviation (RSD) for five repeated measurements of AML (100 μM) on the same day (within-day precision) and over 7 days (day-to-day precision). The RSD values from intra-day and inter-day analysis were found to be 0.58% and 1.6%, respectively. The long-term stability of the CuO-NiO/IL/CPE was evaluated by DPV_S in PB (pH 9, 0.1 M) solution containing AML (100 μM) during two mounts. The result showed the response of electrode did not considerable change. However, renewing of the electrode surface is necessary before each analysis due to poisoning of the electrode surface by adsorption of intermediates or product of electrooxidation. The three different CuO-NiO/IL/CPE_S were prepared at the same conditions the electrode to electrode reproducibility showed a satisfactory RSD value of 4.9% for the determination of AML (100 μM). According to this result, the modified electrodes showed suitable reproducibility in manufacture process and response. A summary of analytical parameters in determination of AML by CuO-NiO/IL/CPE is given in Table 2. The repeatability for 3 replicate determinations of AML 7 μM with the proposed sensor was 4.4%.

Real sample analysis

The standard addition method was performed for determination of AML in real sample. The results show a good recovery for drug determinations as well as the drug declared amounts in the used drug preparations (Table 3). This clearly indicates any interference of the other ingredients and the excipients which are present in the formulations. The results displayed a good recovery for AML determination in human urine and blood plasma samples. The recovery results of the electrochemical sensor were in the range from 97.6 to 102.0% by Eq. 7:

$$Recovery = \frac{Detected}{Added} \times 100 \quad (7)$$

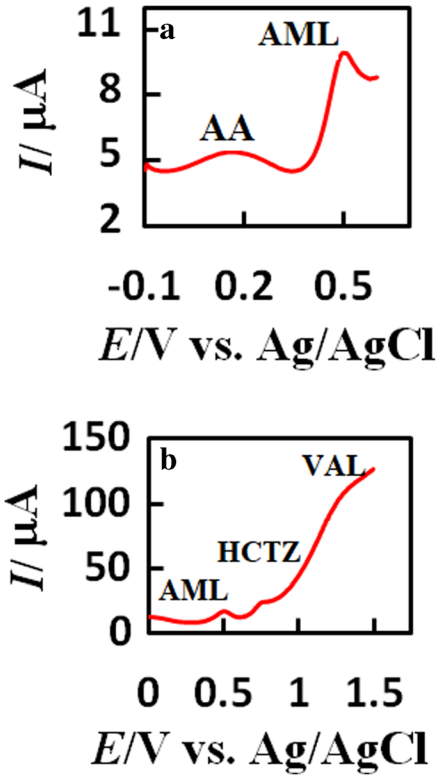

Fig. 9 **a** DPVs of CuO-NiO/IL/CPE in a solution of containing AA (1 mM) and AML (100 µM) in PB (pH 9, 0.1 M). **b** DPVs of CuO-NiO/IL/CPE in a solution of containing AML (100 µM), HCTZ (100 µM), and VAL (100 µM) in PB (pH 9, 0.1 M)

The RSD of three sequential measurements of the response currents AML was found to be about 0.84% by Eq. 8 (Miller and Miller 1993):

Table 2 Analytical parameters of suggested electrode for determination of AML

Linearity range (µM)	0.1–100
Sensitivity (µA/µM)	0.0382
LOD (µM)	0.06
LOQ (µM)	0.21
Mean recovery for real samples (%)	99.64
Repeatability (RSD%) $n = 3$	4.40
Reproducibility (RSD%)	4.90
Within-day precision (RSD%) $n = 5$	0.58
Day-to-day precision (RSD%) $n = 5$	1.60
Bias %	1.22
Stability (day)	60

Table 3 Recovery test of AML determination in real sample

Sample	Standard added (µM)	Found (µM)	Recovery (%)	RSD (%)	Bias (%)
AML 5 mg (Amelodipin ARYA 5)	0	24.4	99.2	0.4	0.8
	5	30.0	101.2	0.7	1.2
	10	34.9	100.8	0.6	0.8
AML:VAL 5:80 mg (Valzomix 5/80 MG TAB)	0	24.4	99.2	0.8	0.8
	5	29.7	100.3	1.0	0.3
	10	34.6	99.9	0.6	0.1
Human blood plasma	5	20.4	102.0	0.6	2
	10	48.8	97.6	0.7	2.4
Urine	5	4.8	97.6	1.7	2.4
	10	9.8	98.6	1.3	1.4

$$RSD = \frac{Sd}{x} \times 100 \quad (8)$$

Conclusions

A modified electrode using the CuO-NiO nanocomposite and BMIM.PF_6 was introduced for the determination of AML in pharmaceutical formulations. The proposed modified electrode exhibited several advantages, including, good mechanical stability, simple preparation high sensitivity, and low cost. These attractive features proved that this proposed electrode is promising for other drug determination.

Acknowledgements This work has been supported by Islamic Azad University South Tehran Branch.

Declarations

Conflict of interest The authors declare no competing interests.

References

Andrieux CP, Saveant JM (1978) Heterogeneous (chemically modified electrodes, polymerelectrodes) vs. homogeneous catalysis of electrochemical reactions. J Electroanal Chem 93:163–168. https://doi.org/10.1016/S0022-0728(78)80230-7

Arvand M, Kaykhaii M, Ashrafi P, Hemmati S (2021) An electrochemical interface for direct analysis of amlodipine in tablets and human blood samples. Mater Sci Eng B 263: 114868. https://doi.org/10.1016/j.mseb.2020.114868

Attala K, Elsonbaty A (2021) Smart UV spectrophotometric methods based on simple mathematical filtration for the simultaneous determination of celecoxib and ramipril in their pharmaceutical mixtures with amlodipine: a comparative statistical study. Pectrochim Acta A Mol Biomol Spectrosc 244:118853. https://doi.org/10.1016/j.saa.2020.118853

Bard AJ, Faulkner L (2001) Electrochemical methods fundamentals and application, vol 1, 2nd edn. Willey, New York

Beitollahi H, Ebadinejad F, Fahimeh S, Torkzadeh Mahani M (2016) Magnetic core–shell Fe_3O_4@SiO_2/MWCNT nanocomposite modified carbon paste electrode for amplified electrochemical sensing of amlodipine and hydrochlorothiazide. Anal Methods 8:6185–6193. https://doi.org/10.1016/j.msec.2013.12.014

Chen PC, Shen G, Zhou C (2008) Chemical sensors and electronic noses based on 1-D metal oxide nanostructures. IEEE Trans Nanotecnol 7:668–682. https://doi.org/10.1109/TNANO.2008.2006273

Chen G, Jirjees F Sr, Bawaba AA, McElnay JC (2018) Quantification of amlodipine in dried blood spot samples by high performance liquid chromatography tandem mass spectrometry. J Chromatogr B 1072:252–258. https://doi.org/10.1016/j.jchromb.2017.11.018

Choi NY, Choi H, Park HH, Lee EH, Yu HJ, Lee KY, Lee YJ, Koh SH (2014) Neuroprotective effects of amlodipine besylate and benidipine hydrochloride on oxidative stress-injured neural stem cells. Brain Res 1551:1–12. https://doi.org/10.1016/j.brainres.2014.01.016

Dehdashti A, Babaei A (2020) Highly sensitive electrochemical sensor based on Pt doped NiO nanoparticles/MWCNTs nanocomposite modified electrode for simultaneous sensing of piroxicam and amlodipine. Electroanalysis 32:1017–1024. https://doi.org/10.1002/elan.201900580

Dogan-Topal B, Bozal B, Demircigil BT, Uslu B, Ozkan SA (2009) Electroanalytical studies and simultaneous determination of amlodipine besylate and atorvastatine calcium in binary mixtures using first derivative of the ratio voltammetric methods. Electroanalysis 21:2427–2439. https://doi.org/10.1002/elan.200904689

Dollery C (1999) Therapeutic drugs, 2nd edn. Churchill Livingstone, UK, p 151

Doulache M, Bakirhan NK, Saidat B, Ozkan SA (2020) Highly sensitive and selective electrochemical sensor based on polyglycine modified glassy carbon electrode for simultaneous determination of amlodipine and ramipril from biological samples. J Electrochem Soc 167:027511. https://doi.org/10.1149/issn.1945-7111

Erden PE, Tasdemir IH, Kaçar C, Kiliç E (2014) Simultaneous determination of valsartan and amlodipine besylate in human serum and pharmaceutical dosage forms by voltammetry. Int J Electrochem Sci 9:2208–2220

Erden S, Bayraktepe DE, Yazan Z, Dinc E (2016) TiO_2 modified carbon paste sensor for voltammetric analysis and chemometric optimization approach of amlodipine in commercial formulation. Ionics 22:1231–1240. https://doi.org/10.1007/s11581-015-1629-2

Fares H, DiNicolantonio JJ, O'Keefe JH, Lavie1 CJ (2016) Amlodipine in hypertension: a first-line agent with efficacy for improving blood pressure and patient outcomes. Open Heart 3: e000473. https://doi.org/10.1136/openhrt-2016-000473

Farvardin N, Jahani S, Kazemipour M, Foroughi MM (2020) The synthesis and characterization of 3D mesoporous CeO2 hollow spheres as a modifier for the simultaneous determination of amlodipine, hydrochlorothiazide and valsartan. Anal Methods 12:1767–1778. https://doi.org/10.1039/D0AY00022A

Goyal RN, Bishnoi S (2010) Voltammetric determination of amlodipine besylate in human urine and pharmaceuticals. Bioelectrochemistry 79:234–240. https://doi.org/10.1016/j.bioelechem.2010.06.004

Jadon N, Jain R, Pandey A (2017) Electrochemical analysis of amlodipine in some pharmaceutical formulations and biological fluid using disposable pencil graphite electrode. J Electroanal Chem 788:7–13. https://doi.org/10.1016/j.jelechem.2017.01.055

Johannsen JO, Reuter H, Hoffmann F, Blaich C, Wiesen MHJ, Streichert T, Müller C (2019) Reliable and easy-to-use LC-MS/MS method for simultaneous determination of the antihypertensives metoprolol, amlodipine, canrenone and hydrochlorothiazide in patients with therapy-refractory arterial hypertension. J Pharm Biomed Anal 5:373–381. https://doi.org/10.1016/j.jpba.2018.11.002

Kearney M, Whelton M, Reynolds K, Muntner P, Whelton PK, He J (2005) Global burden of hypertension: analysis of worldwide. Lancet 365:217–223. https://doi.org/10.1016/S0140-6736(05)17741-1

Lou B-S, Rajaji U, Chen S-M, Chen T-W (2020) A simple sonochemical assisted synthesis of porous NiMoO4/chitosan nanocomposite for electrochemical sensing of amlodipine in pharmaceutical formulation and human serum. Ultrason Sonochem 64:104827. https://doi.org/10.1016/j.ultsonch.2019.104827

Miller JC, Miller JN (1993) Statistics for analytical chemistry, 3rd edn. Ellis Horwood Ltd.

Mirzaei A, Leonardi SG, Neri G (2016) Detection of hazardous volatile organic compounds (VOCs) by metal oxide nanostructures-based gas sensors: a review. Ceram Int 42: 15119–15141. https://doi.org/10.1016/j.ceramint.2016.06.145

Mohammadi N, Najafi M, Bahrami Adeh N (2017) Highly defective mesoporous carbon–ionic liquid paste electrode as sensitive voltammetric sensor for determination of chlorogenic acid in herbal extracts. Sensors Actuators B Chem 243:838–846. https://doi.org/10.1016/j.snb.2016.12.070

Mohammadizadeh N, Mohammadi SZ, Kaykhaii M (2017) Novel electrochemical sensor based on ZrO_2 nanoparticles modified glassy carbon electrode for low-trace level determination of amlodipine by differential pulse voltammetry. Anal Bioanal Electrochem 9:390–399

Naghian E, Najafi M (2018) Carbon paste electrodes modified with SnO_2/CuS, SnO_2/SnS and Cu@SnO_2/SnS nanocomposites as voltammetric sensors for paracetamol and hydroquinone. Microchim Acta 185:406. https://doi.org/10.1007/s00604-018-2948-6

Naikoo GA, Pandit UJ, Sheikh MUD, Hassan IU, Khan GA, Bhat AR, Das R, Horchani R (2020) Synergistic effect of carbon nanotubes, copper and silver nanoparticles as an efficient

electrochemical sensor for the trace recognition of amlodipine besylate drug. N Appl Sci 2:983. https://doi.org/10.1007/s42452-020-2807-z

Opallo M, Lesniewski A (2011) A review on electrodes modified with ionic liquids. J Electroanal Chem 15:2–16. https://doi.org/10.1016/j.jelechem.2011.01.008

Reddy CV, Reddy KR, Shetti NP, Shim J, Aminabhavi TM, Dionysiou DD (2020) Hetero-nanostructured metal oxide-based hybrid photocatalysts for enhanced photoelectrochemical water splitting—a review. Int J Hydrog Energy 45:18331–18347. https://doi.org/10.1016/j.ijhydene.2019.02.109

Shaikh JSA, Raut S, Bdul AA, Pathan MAAK (2020) High performance liquid chromatographic assay of amlodipine, valsartan and hydrochlorothiazide simultaneously and its application to pharmaceuticals urine and plasma analysis. J Chromatogr B 1155:122295. https://doi.org/10.1016/j.jchromb.2020.122295

Stoiljković Z, Avramov Ivić M, Petrović SD, Mijin D, Stevanović S, Lačnjevac U, Marinković A (2012) Voltammetric and square-wave anodic stripping determination of amlodipine besylate on gold electrode. Int J Electrochem Sci 7:2288–2303

Švorc LU, Cinková K, Sochr J, Vojs M, Michniak P, Marton M (2014) Sensitive electrochemical determination of amlodipine in pharmaceutical tablets and human urine using a boron-doped diamond electrode. J Electroanal Chem 728:86–93. https://doi.org/10.1016/j.jelechem.2014.06.038

United States Pharmacopoeia (2009) United States Pharmacopoeial Convention. Rockville